THERMO-CATALYTIC PYROLYSIS OF LIGNOSULFONATE FROM THE SULFITE PROCESS

**Gabriel VASILIEVICI[a], Andreea-Luiza MÎRŢ[a,b,*],
Simona-Bianca GHIMIȘ[a], Grigore PȘENOVSCHI[a,b], Mihai SÎRBU[c]**

ABSTRACT. This paper shows the results of thermal and catalytic pyrolysis of conditioned lignosulfonate from the sulfite process, with a specific focus on the analysis of bio-oil and biochar. The conditioning of lignosulfonate was made by drying and grinding in a planetary ball mill. Thermal and catalytic pyrolysis of conditioned lignosulfonate were carried out under the same temperature and flow conditions. The use of two different catalysts produced via the impregnation method has shown distinctive effects, influencing both bio-oil yield and chemical composition. The resulting biochar exhibits characteristics comparable to non-activated carbonaceous materials, with variations in its specific surface area and pore size depending on the catalyst.

Keywords: catalytic pyrolysis, lignosulfonate, sulfite process, bimetallic catalyst

INTRODUCTION

Catalytic biomass pyrolysis is a promising technology for the efficient utilization of biomass, converting it into high-quality liquid fuels and chemicals in a single reactor and through a single step [1-3]. In the absence of oxygen, at high temperatures, organic matter undergoes thermochemical decomposition

[a] *National Institute for Research & Development in Chemistry and Petrochemistry–ICECHIM, 202 Spl. Independentei, 060021 Bucharest, Romania*
[b] *Faculty of Chemical Engineering and Biotechnologies, University Politehnica of Bucharest, 1-7 Polizu Street, 011061 Bucharest, Romania*
[c] *CCH – The Cellulose and Paper Plant, 2 Nicolae Iorga Bvd., Drobeta-Turnu Severin 220236, Mehedinti, Romania*
[*] *Corresponding author: luiza.mirt@icechim.ro*

known as pyrolysis or destructive distillation, resulting biochar, liquid part bio-oil and gases [4]. The term "pyrolysis" has its roots in the Greek language, where "pyro" means "fire," and "lysis" translates as "separation" [5].

In the pursuit of valorizing secondary streams from industrial processes, pulp and paper mills are striving to optimize their biomass utilization. Spent sulfite liquor, also known as red liquor, constitutes a waste byproduct of the sulfite process employed in cellulose production from lignocellulosic biomass [6]. This biomass, a fundamental resource for paper and regenerated cellulose fiber manufacturing, undergoes a sulfite-based treatment to yield high-quality cellulose through lignin and hemicellulose removal [7-8].

The resultant red liquor is notably rich in monomeric sugars and lignosulfonates, historically exploited as a substrate for industrial-grade ethanol production [9].

Pyrolysis involves the rapid and simultaneous depolymerization and fragmentation of biomass components such as cellulose, hemicellulose, and lignin, bio-oil is generated [10]. The resulting pyrolysis oil, also known as bio-oil, can be obtained with impressive yields of up to 70-80% by weight, contingent upon the proportions of cellulose and lignin present in the wood material [11]. Bio-oil, a microemulsion, consists of two phases: one is an aqueous solution containing decomposition products of cellulose, hemicellulose and smaller molecules from lignin decomposition, while the other primarily comprises pyrolytic lignin macromolecules [12].

Due to the significant content of oxygenated compounds, particularly lignin derivatives, bio-oils possess relatively low heating values, exhibit inherent instability, high viscosity, low volatility, and corrosive properties. As certain lignin oligomers resist vaporization during pyrolysis, comprehensive identification of all compounds using GC-MS analysis, poses challenges [13-15]. Consequently, the upgrading of bio-oil is necessary to improve its properties prior to utilization [16-17].

The solid residue produced during pyrolysis, known as biochar, primarily comprises carbon (approximately 85%), along with oxygen and hydrogen. It retains a significant portion of the inorganic components found in the original biomass [11]. Biochar holds considerable value as a by-product and can serve various purposes, including as a solid fuel for boilers, utilized in processes such as steam reforming or thermal cracking to generate hydrogen or syngas [18-19] and as a medium for filtering and adsorbing both organic and inorganic pollutants [3, 20-22].

Catalytic pyrolysis of lignosulfonate from the sulfite process for the production of aromatic compounds such as BTX (benzene, toluene, xylene) has been conducted using modified H-ZSM-5 zeolite catalysts with Ga, Mo, and Zn in microreactors under inert gas atmosphere, as reported in literature [23-24].

However, the catalysts' lifespan is limited due to carbonaceous material formation. The irreversible deactivation of the acidic sites by inorganic cations (Na^+, K^+, Ca^{2+}) present in high concentrations in the feedstock poses a significant challenge, leading to decreased acidity and subsequently lower conversion to aromatic compounds [25].

In co-processing studies of lignosulfonate and plastic waste (polyolefins and polystyrene) in fluidized bed reactors, catalysts for olefin cracking, catalytic cracking catalysts (such as ZSM-5), and gamma-alumina have been employed [26-27].

Catalytic pyrolysis of lignin in the presence of catalysts such as NiO, MoO_2, and Co_3O_4 has the potential to inhibit bio-char formation and enhance the properties of bio-oil by reducing the concentration of oxygenated compounds hours [28-29]. The addition of catalysts leads to increased bio-oil yield, particularly in the presence of 10% added hydrogen in the inert atmosphere. The bio-oil yield increased by 26.38% through catalytic pyrolysis using Co_3O_4 catalyst in an H_2/N_2 atmosphere [30].

This paper presents innovative processes for lignosulfonate process by pyrolysis. Catalytic pyrolysis was carried out in the presence of new catalysts obtained by the impregnating method of Mo and Ni precursors on alumina support. The study explores the potential of catalytic pyrolysis as a conversion method for transforming lignosulfonate from sulfite process into valuable products.

RESULTS AND DISCUSSION

Lignosulfonate characterization

The lignosulphonate used in the experimental programme was derived from waste liquor generated during the production of wood pulp through the sulphite process. The raw lignosulfonate sample was analyzed by determining the dry matter content after water removal, ash content (calcination residue) and thermal analysis (thermogravimetric analysis TGA).

Table 1. Characterization of lignosulfonate samples

Sample	Dry substance content, %	Calcination residue, %	pH
Lignosulfonate	52.56	37.54%	8.20 (25ºC)

GABRIEL VASILIEVICI, ANDREEA-LUIZA MÎRȚ, SIMONA-BIANCA GHIMIȘ,
GRIGORE PȘENOVSCHI, MIHAI SÎRBU

The thermogravimetric analysis shows the thermal behavior of the sample, revealing distinct mass loss patterns at various temperature ranges. Initially, a mass loss of 6.05% is observed up to 140ºC, which can be attributed to the presence of water and volatile components in the sample. Subsequently, within the temperature range of 180-550ºC, the mass loss curve exhibits three distinct peaks at 218.3ºC, 270.4ºC, and 395.0ºC. These peaks correspond to the decomposition of hemicellulose and lignin [31]. The cumulative mass loss associated with these peaks yields an organic matter content of 37.48% within the solid portion of the sample lignosulfonate. Furthermore, the residue obtained at 750ºC under ambient air conditions is recorded as 47.61%.
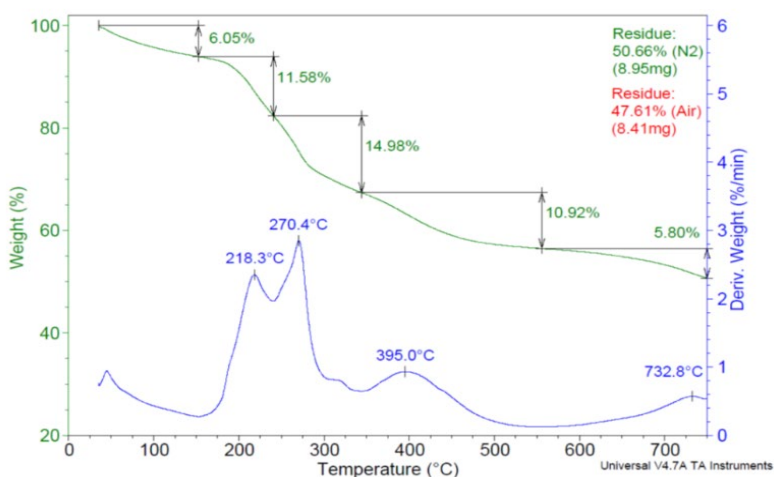

Figure 1. Thermogravimetric analysis of lignosulfonate

Conditioning lignosulfonate samples

The lignosulfonate samples were conditioned before pyrolysiss by drying in a circulating air oven and then grinding in a planetary ball mill.

The resulting lignosulfonate powder was analyzed by DLS method (dynamic light scattering) to evaluate the particle size of lignosulfonate and size distribution. The lignosulfonate particles are polydisperse, forming large aggregates, the results being presented in table 2 and figure 2.

Table 2. Characteristics of lignosulfonate particles

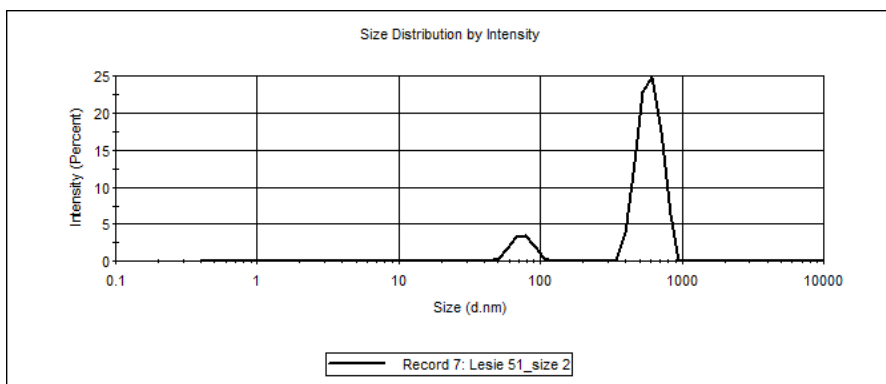| Sample	Dm (nm)	PdI	Observations
Lignosulfonate	1337	0.820	Polydisperse, contains numerous large aggregates, with dimensions > 6µm

Figure 2. Particle size distribution as a function of intensity

Catalyst characterization

The structural characteristics of the catalysts were examined using nitrogen porosimetry and are presented in Table 3. Prior to analysis, the catalyst samples were subjected to a vacuum degassing process for 4 hours at 160ºC. The resulting catalysts are mesoporous materials with pore diameters ranging from 4 nm to 10 nm.

Table 3. Characteristics of catalysts

No.	Catalyst name	Specific surface, m^2/g	Total pore volume, cm^3/g	Average pore diameter, nm
2	Mo/Al$_2$O$_3$	157.3	0.244	6.207
3	NiMo/Al$_2$O$_3$	236.8	0.2839	4.795

Thermal pyrolysis of lignosulfonate

The analysis of the bio-oil obtained by thermal pyrolysis of conditioned lignosulfonate is presented in Table 4 and Figure 3. The GC-MS chromatogram shows a multitude of peaks. The liquid phase's composition show the presence of oxygenated compounds with an aromatic structure - phenols and substituted phenols, linear and cyclic oxygenated aliphatic compounds, including carbonyl compounds, acids, and alcohols.

Table 4. GC-MS analysis of bio-oil pyrolysis of lignosulfonate without catalyst

| Peak Number	Retention Time	Compounds name
1	5.335	2-Butanone, 3-hydroxy-
2	5.551	Acetic anhydride
3	6.460	2-Hepten-1-ol, (E)-
4	7.322	Acetic acid
5	7.561	2-Propanone, 1-(acetyloxy)-
6	9.484	Butanoic acid
7	9.907	Furfuryl alcohol
8	11.415	1,3-Cyclopentanedione, 2,4-dimethyl-
9	11.495	Cyclohexanone, 2-acetyl-
10	11.822	2-Cyclopenten-1-one, 2-hydroxy-3-methyl-
11	12.029	Cyclohexanone, 2-acetyl-
12	12.173	Phenol, 2-methoxy-
13	13.649	Phenol
14	16.146	Phenol, 2,6-dimethoxy-
15	19.473	2-Propanone, 1-(4-hydroxy-3-methoxyphenyl)-
16	23.646	Desaspidinol
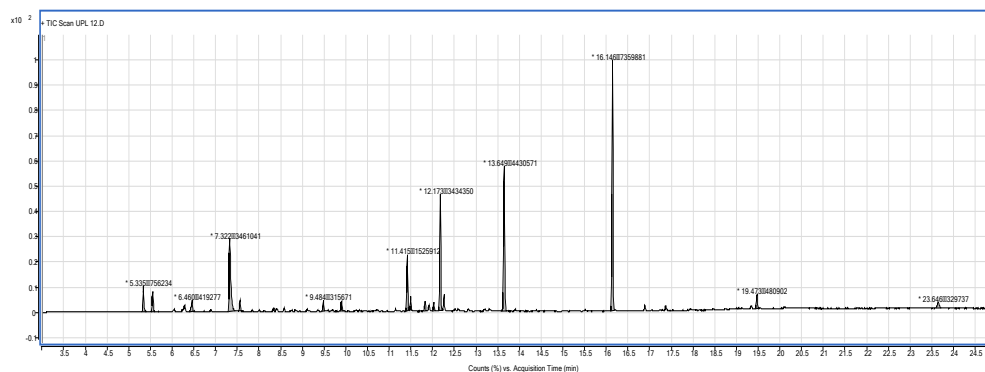
Figure 3. Chromatogram of bio-oil pyrolysis of lignosulfonate without catalyst

The porosimetry data of biochar was obtained by nitrogen adsorption measurements with NOVA 2200e-Quantachrome apparatus. The obtained results showed that pyrolyzing the residues yields carbonaceous materials characterized by a reduced specific surface area and pore volume, yet retaining

adsorption capabilities for chemical compounds. Conversely, biochar possessing an increased surface area is considered more porous, which makes it appropriate for applications like water treatment and environmental remediation [32-33].

Table 5. Porosimetry characteristics of biochar

No.	Sample name	Specific surface, m^2/g	Total pore volume, cm^3/g	Average pore diameter, nm
1	Biochar	1.982	0.0045	9.101

Catalytic pyrolysis of lignosulfonate

The GC-MS analysis of the bio-oil produced using Mo/Al$_2$O$_3$ are shown in Table 6 and Figure 5. The homogenization of the catalyst and conditioned lignosulfonate particles was done by grinding them together in the planetary ball mill.

Table 6. GC-MS analysis of bio-oil pyrolysis in the presence of Mo/Al$_2$O$_3$

| Peak Number	Retention Time	Compounds name
1	4.745	2-Butanone, 3-hydroxy-
2	4.929	2-Propanone, 1-hydroxy-
3	5.567	Furan, 3-methyl-
4	6.253	Acetic acid
5	6.684	1,2-Ethanediol, diacetate
6	7.474	Propanoic acid
7	7.681	2-Cyclopenten-1-one, 2,3-dimethyl-
8	8.511	Butanoic acid
9	10.434	1,3-Cyclopentanedione, 2,4-dimethyl-
10	11.192	Phenol, 2-methoxy-
11	12.644	Phenol
12	12.915	Phenol, 4-ethyl-2-methoxy-
13	15.174	Phenol, 2,6-dimethoxy-
14	15.892	Phenol, 4-methoxy-3-(methoxymethyl)-
15	16.370	Benzene, 1,2,3-trimethoxy-5-methyl-
16	18.477	2-Propanone, 1-(4-hydroxy-3-methoxyphenyl)-
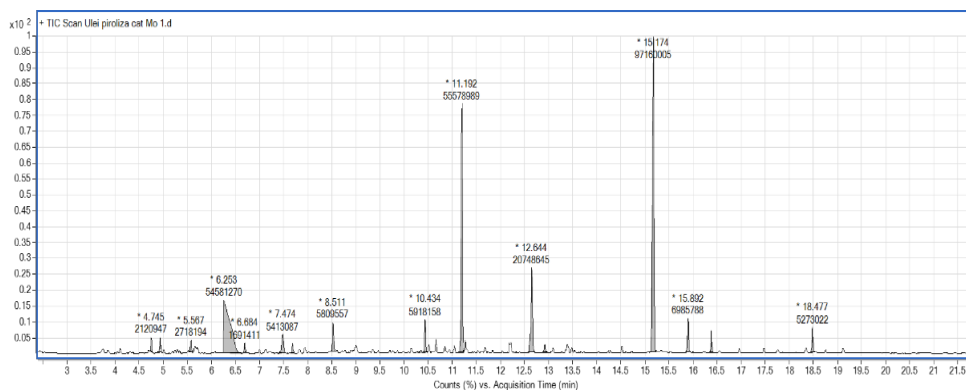
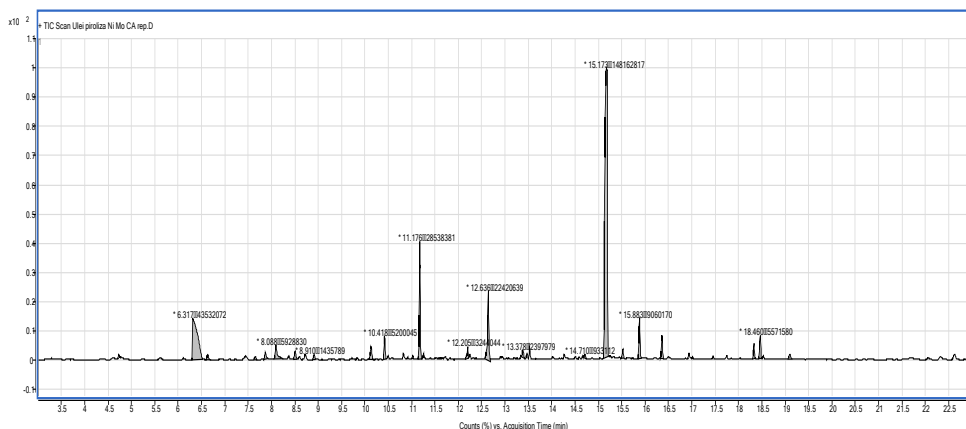**Figure 4.** Chromatogram of bio-oil pyrolysis in the presence of Mo/Al$_2$O$_3$

Figure 5. Chromatogram of bio-oil pyrolysis in the presence of Ni-Mo/Al$_2$O$_3$

A catalytic pyrolysis was performed using a nickel and molybdenum based bimetallic catalyst. The results acquired through GC-MS analysis of the bio-oil are shown in Table 7 and Figure 6. This bio-oil analysis resulting from catalytic pyrolysis shows the presence of numerous aromatic compounds, compared to conventional pyrolysis. This enhancement can be attributed to the catalytic active sites that facilitate the deoxygenation of compounds within the lignosulfonate [34-35].

Table 7. GC-MS analysis f bio-oil pyrolysis in the presence of Ni-Mo/Al$_2$O$_3$

Peak Number	Retention Time	Compounds name
1	6.317	Acetic acid
2	6.628	2-Propanone, 1-(acetyloxy)-
3	7.649	2-Cyclopenten-1-one, 2,3-dimethyl-
4	7.872	2-Propanone, 1-hydroxy-
5	8.088	Propylene Glycol
6	8.503	Butanoic acid
7	8.910	2-Furanmethanol
8	10.130	Acetamide
9	10.418	1,3-Cyclopentanedione, 2,4-dimethyl-
10	11.176	Phenol, 2-methoxy-
11	12.205	1,2,3 Trimethoxybenzene
12	12.636	Phenol
13	13.378	Phenol, 2,4-dimethyl-
14	14.710	Phenol, 2-ethyl-4-methyl-
15	15.173	Phenol, 2,6-dimethoxy-
16	15.524	Phenol, 2,6-dimethoxy-, acetate
17	15.883	1,2,4-Trimethoxybenzene
18	16.362	Benzene, 1,2,3-trimethoxy-5-methyl-
19	18.333	Ethanone, 1-(4-hydroxy-3-methoxyphenyl)-
20	18.460	2-Propanone, 1-(4-hydroxy-3-methoxyphenyl)-
21	19.099	Phenol, 2,6 - dimethoxy -4-(2-propenyl)

Utilizing GC-MS analysis, it was found that the liquid phase includes oxygenated compounds characterized by aromatic structures, phenolic compounds, furans, substituted benzene and linear/cyclic aliphatic oxygenated compounds - carbonyl compounds and organic acids. It was observed that the presence of a Mo-based catalyst during pyrolysis resulted in a higher concentration of organic acids and a higher concentration of furanic compounds compared to a Ni-Mo based catalyst. The obtained results supports the findings reported in the literature [36]. Molybdenum-based catalysts exhibit C-C bond cleavage in the side chains, leading to significant production of carboxylic compounds [37-38]. Adding nickel, in contrast, suppresses the reaction between aromatics and other oxygenated substances, yielding a variety of alkylated aromatic compounds [39-40].

Table 8. Overview of the results from pyrolysis experiments

Identified compounds	Without catalyst	Mo catalyst, %	Ni-Mo catalyst, %
Furanic compounds	1.15	0.99	0.48
Aliphatic ketones	15.77	6.47	7.77
Organic acids	15.42	24.03	17.29
Phenolic compounds	62.17	66.46	68.76
Other compounds	5.49	2.06	5.70

Table 9 below shows the characteristics of biochar, which has similar attributes of non-activated carbons. Moreover, the presence of molybdenum-based catalysts during pyrolysis reactions partially contributes to the destruction of the biochar's micropores. Bimetallic catalysts often display a synergistic effect, significantly increasing the pyrolysis reaction, especially when compared to monometallic catalysts [41]. The pyrolysis with bimetallic catalysts resulted in materials with higher specific surface area and pore volume compared to the use of monometallic catalysts (approximately 7 times larger), accompanied by a 50% reduction in average pore size.

Table 9. Porosimetry analysis of biochar

No.	Catalyst	Specific surface, m^2/g	Total pore volume, cm^3/g	Average pore diameter, nm
1	Biochar with Mo/Al_2O_3 catalyst	0.40	0.0020	20.19
2	Biochar with $Ni-Mo/Al_2O_3$ catalyst	15.59	0.0269	6.90

CONCLUSION

This study presents the conditioning of lignosulfonate from the sulfite method used in the production of cellulose from lignocellulosic biomass and thermal and catalytic pyrolysis of conditioned lignosulfonate, focusing on the production and analysis of bio-oil and biochar. The obtained results provide valuable insights into the impact of catalytic pyrolysis of lignosulfonate and its potential applications. The utilization of molybdenum and nickel-molybdenum catalysts showcased distinctive effects on the bio-oil yield, chemical composition and product distribution. The GC-MS analysis revealed various compounds, including oxygenated species like phenols, furans, aliphatic compounds, and carbonyl compounds within the liquid phase of the bio-oil. Porosimetric analysis of the biochar resulting from pyrolysis shows the catalyst's role in determining biochar porosity. The presence of molybdenum catalyst leads to biochar with

reduced specific surface area, whereas the utilization of a nickel-molybdenum-based catalyst substantially enhances it. The effects of using catalytic pyrolysis compared to non- catalytic pyrolysis to recycle the lignosulfonate residue and to characterise the materials obtained from this process are presented.

EXPERIMENTAL PART

Lignosulfonate characterization

The gravimetric method was used to determine the dry substance content of lignosulfonate samples. Water was removed from the samples by subjecting them to heat in an air circulation oven at 85ºC for 8 hours, followed by further heating at 105ºC for 16 hours. Subsequently, the samples were heated to 100ºC under a vacuum of 4 mmHg pressure until a constant mass was achieved. To assess the pH of lignosulfonate, a portable pH-meter model 1140 (Mettler Toledo Gmbh-Switzerland) was utilized, with measurements at room temperature (25ºC).

For the evaluation of the ash content (calcination residue), the solid fraction of the red liquor, obtained through calcination in a furnace, was employed. The temperature of the furnace was gradually increased from room temperature to 850ºC, with a heating rate of 5ºC/min. Intermediate steps at 250ºC and 500ºC were incorporated, each lasting 2 hours. The resulting residue was then correlated with the dry substance content of the lignosulfonate samples.

Thermogravimetric analysis (TGA) was performed with a TA Q5000 (TA Instruments, New Castle, DE, USA). The sample, approx. 17.6 mg - the solid part of the red liquor sample, was heated from room temperature to 750ºC at a heating rate of 10ºC/min in an inert gas (nitrogen) atmosphere at a flow rate of 50 mL/min recording mass changes; and switching the inert gas with synthetic air at 750ºC to record the residue resulted in air.

Conditioning of lignosulfonate

The lignosulfonate samples were conditioned in two steps before pyrolysiss. First step involve drying in an circulating air oven at 85ºC for 8 hours, followed by heating at 105ºC for 16 hours.

Second step was grinding of lignosulfonate in a planetary ball mill, Retsch PM100 from Retsch GmbH, Haan, Germany, with Φ10mm stainless steel balls in a 125 ml stainless steel grinding jar.

The measurement of lignosulfonate particles was conducted using a particle size measurement system comprising a Zetasizer Nano ZS instrument (Red badge) from Malvern Instruments Ltd.,UK, and a computer with Zetasizer

software for sample measurement control. The Zetasizer Nano instruments perform particle size measurements using the technique Dynamic Light Scattering (DLS) [42]. This measures fluctuations in the intensity of scattered light and uses these fluctuations to calculate the size of the particles in the sample. DLS measures Brownian motion and correlates it with particle size.

Particles suspended in a liquid undergo continuous movement due to Brownian motion, so smaller particles move faster and larger particles move slowly. When larger particles, which move more slowly, are measured, the intensity of scattered light will vary gradually. Similarly, for smaller particles, since they move very quickly, the intensity of scattered light will also fluctuate rapidly [42-44]. For the DLS analysis the samples were prepared as follows: 0.2 mL sample was diluted to the mark with distilled water in a 25 mL volumetric flask. For each sample a minimum of 5 measurements were performed and the measurement with the values closest to the mean value was selected.

Catalyst preparation and characterization

Catalysts for pyrolysis were prepared in the laboratory through the impregnation method.The catalysts were synthesized employing the wet impregnation method on the alumina powder support, using aqueous solutions of $MoO \cdot 3H_2O$ and $Ni(NO_3)_2 \cdot 6H_2O$. The metallic precursors, dissolved in the aqueous ammonia solution, were incorporated into the solutions of $MoO_3 \cdot H_2O$ and $Ni(NO_3)_2 \cdot 6H_2O$ under continuous stirring. Subsequently, the resultant mixture was used for the support impregnation at room temperature. The impregnated sample was air-dried overnight at room temperature, followed by additional drying in a 120°C air circulation oven for 12 hours. The last step was calcination in a furnace at 450°C for 5 hours. The prepared catalysts were named Mo/Al_2O_3, and $Ni-Mo/Al_2O_3$.

The textural characteristics of catalysts and biochars were analysed by nitrogen adsorption measurements with NOVA 2200e-Quantachrome apparatus from Quantachrome Instruments, USA. Analysis of data was conducted using NovaWin software ver. 11.03. All the samples were vacuum degassed before analysis at 300°C for 4 h.The specific surface area was determined through the B.E.T. (Brunauer-Emmett-Teller) method by analyzing the linear plot of the adsorption isotherm. Total pore volume and pore size distribution were estimated based on the adsorbed N_2 quantity. The total pore volume was calculated from single-point adsorption at a relative pressure near unity, while the average pore diameter was derived from the adsorption average pore diameter using the surface area determined through the B.E.T. method.

Pyrolysis

The pyrolysis reactor used in processing the lignosulfonate has a horizontal, batch-operated configuration, composed of stainless steel, with an inner diameter of Ø 25.4mm and a length of 250mm. The reactor integrates a thermocouple for internal temperature measurement. For heating, a digitally controlled electric oven at external wall thermocouple is employed.

Before each experiment, inert gas (nitrogen) is purged into the reactor to remove oxygen. The pyrolysis reactor was fed with a homogenized mixture of lignosulfonate with 1% catalyst, prepared by grinding in a planetary ball mill. Figure 7 shows a schematic representation of the pyrolysis reactor, where inert gas flow is regulated using a mechanical valve and a flow meter. The resulting pyrolysis products undergo cooling in a heat exchanger and subsequently enter a gas-liquid separator. The liquid fraction is collected, prepared, and subjected to analysis by gas chromatography (GC-MS).
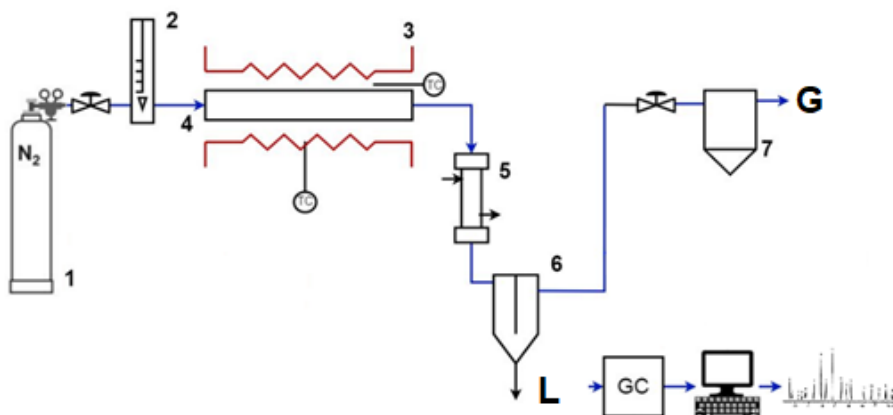

Figure 6. Schematic representation of pyrolysis reactor. 1-inert gas cylinder, 2-flow meter, 3- electric heating oven, 4- pyrolysis reactor, 5-heat exchanger (cooler), 6- gas-liquid separator, 7-gas container, TC- thermocouple and heat display system, GC- gas chromatograph

The pyrolysis reactions were conducted at 500°C for 4 hours, with the reactor ramped up to the operational temperature at a rate of 20°C/min. The mixture of conditioned lignosulfonate and catalyst was grinded and subsequently introduced into the reactor within ceramic nacelles. The catalyst concentration was maintained at 2% (mass) relative to the lignosulfonate mass.

GABRIEL VASILIEVICI, ANDREEA-LUIZA MÎRȚ, SIMONA-BIANCA GHIMIȘ,
GRIGORE PȘENOVSCHI, MIHAI SÎRBU

Bio-oil characterization

The liquid fraction's characterization was performed using GC-MS analysis with Agilent 7890 A GC-MS/MS TRIPLE QUAD system. A DB-WAX capillary column from Agilent (30 m length, 0.25 mm internal diameter, 0.25 µm film thickness) was utilized, with helium as the carrier gas flowing at 1 mL/min. The initial oven temperature was 70°C, gradually increased to 230°C at a rate of 4°C/min, holding for 5 minutes. The GC injector temperature was 250°C, while the MS detector was set to 150°C. The transfer line temperature was maintained at 280°C. MS detection occurred in the electron ionization (EI) mode at 70 eV, with a mass scanning range of m/z 50-450. The NIST MS database facilitated peak identification within the analyzed samples.

ACKNOWLEDGMENTS

REFERENCES

1. T. Y. A. Fahmy, Y. Fahmy, F. Mobarak, M. El-Sakhawy, R. E. Abou-Zeid; *Environ. Dev. Sustain.*, **2018**, *22 (1)*, 17-32.
2. H. Zhang, R. Xiao, J. Nie, B. Jin, S. Shao, G. Xiao; *Bioresour. Technol.*, **2015**, *192*, 68-74.
3. V. Goia, C.-C. Cormoş, P. Ş. Agachi; *Studia UBB Chemia*, **2011**, *56 (2)*, 49-56.
4. J. König, L. Walleij; Inst. Trätekn. Forskn., Stockholm, **1999**.
5. B. Östman; *Wood Mater. Sci. Eng.,* **2021**, *17 (1)*, 2-5.
6. R. Janzon, J. Puls, B. Saake; *Holzforschung*, **2006**, *60 (4)*, 347-354.
7. R. Hoheneder, E. Fitz, R. H. Bischof, H. Russmayer, P. Ferrero, S. Peacock, M. Sauer; *Bioresour. Technol.*, **2021**, *333*, 125215.
8. J. A. Sirvio, M. Mikola, J. Ahola, J. P. Heiskanen, S. Filonenko, A. Ammala; *Carbohydr. Polym.*, **2023**, *312*, 120815.
9. Z. Guo, L. Olsson; *Process Biochem.*, **2014**, *49 (8)*, 1231-1237.
10. G. Lyu, S. Wu, H. Zhang; *Front. Energy Res.*, **2015**, 3.
11. P. Basu; in Biomass Gasification, Pyrolysis, Torrefaction, **2013**; pp 147-176.
12. D. S. Scott, J. Piskorqt, M. A. Bergougnou, R. Graham, R. P. Overend; *Ind. Eng. Chem. Res.*, **1988**, *27*, 8-15.

13. C. Gerdes, C. M. Simon, T. Ollesch, D. Meier, W. Kaminsky; *Eng. Life Sci*., **2002**, *2 (6)*, 167-174.
14. Z. Zhang, D. J. Macquarrie, M. De bruyn, V. L. Budarin, A. J. Hunt, M. J. Gronnow, J. Fan, P. S. Shuttleworth, J. H. Clark, A. S. Matharu; *Green Chem*., **2015**, *17 (1)*, 260-270.
15. Q. Lu, Z.-b. Zhang, X.-c. Yang, C.-q. Dong, X.-f. Zhu; *J. Anal. Appl. Pyrolysis*, **2013**, *104*, 139-145.
16. T. Stoikos; in Biomass Pyrolysis Liquids Upgrading Utilization, A. V. Bridgwater, Ed., Elsevier Appl. Sci., **1991**.
17. Pattiya; in Direct Thermochem. Liquefaction Energy Appl., **2018**; pp 3-28.
18. H. B. Goyal, D. Seal, R. C. Saxena; *Renew Sust Energ Rev*., **2008**, *12 (2)*, 504-517.
19. G. W. Huber, S. Iborra, A. Corma; *Chem. Rev*., **2006**, *106*, 4044−4098.
20. L. Delgado-Moreno, S. Bazhari, G. Gasco, A. Mendez, M. El Azzouzi, E. Romero; *Sci. Total Environ*., **2021**, *752*, 141838.
21. D. Mohan, A. Sarswat, Y. S. Ok, C. U. Pittman Jr.; *Bioresour. Technol*., **2014**, *160*, 191-202.
22. M. Ahmad, A. U. Rajapaksha, J. E. Lim, M. Zhang, N. Bolan, D. Mohan, M. Vithanage, S. S. Lee, Y. S. Ok; *Chemosphere*, **2014**, *99*, 19-33.
23. D. J. Mihalcik, C. A. Mullen, A. A. Boateng; *J. Anal. Appl. Pyrolysis*, **2011**, *92 (1)*, 224-232.
24. A. Heeres, N. Schenk, I. Muizebelt, R. Blees, B. De Waele, A. J. Zeeuw, N. Meyer, R. Carr, E. Wilbers, H. J. Heeres; *ACS Sustainable Chem. Eng*., **2018**, *6 (3)*, 3472-3480.
25. A. Palčić, V. Valtchev; *Appl. Catal*., **2020**, *606*, 117-795.
26. A. Nechita Rotta, C. Bota, B. Brém, D. I. Porumb, E. Gál; *Studia UBB Chemia*, **2022**, *67 (4)*, 169-185.
27. M. Sajdak, R. Muzyka; *J. Anal. Appl. Pyrolysis*, **2014**, *107*, 267-275.
28. F. Liu, S. Xu, L. Cao, Y. Chi, T. Zhang, D. Xue; *J. Phys. Chem. C*, **2007**, *111*, 7396-7402.
29. Q. Wei, P. Zhang, X. Liu, W. Huang, X. Fan, Y. Yan, R. Zhang, L. Wang, Y. Zhou; *Front. Chem*., **2020**, *8*, 586445.
30. J. Chen, C. Liu, S. Wu, J. Liang, M. Lei; *RSC Adv*., **2016**, *6 (109)*, 107970-107976.
31. R. Sun, J. Tomkinson, G. L. Jones; *Polym. Degrad. Stabil*., **2000**, *68*, 111-118.
32. S. Roy, U. Kumar, P. Bhattacharyya; *Environ Sci Pollut Res Int*, **2019***, 26 (7)*, 7272-7276.
33. Z. Chen, T. Liu, J. Tang, Z. Zheng, H. Wang, Q. Shao, G. Chen, Z. Li, Y. Chen, J. Zhu, T. Feng; *Environ Sci Pollut Res Int*, **2018**, *25 (12)*, 11854-11866.
34. M. d. C. Rangel, F. M. Mayer, M. d. S. Carvalho, G. Saboia, A. M. de Andrade; *Biomass*, **2023**, *3 (1)*, 31-63.
35. X. Lu, X. Gu; *Biotechnol Biofuels Bioprod*, **2022**, *15 (1)*, 106.
36. P. Straka, O. Bičáková, T. Hlinčík; *Catalysts*, **2021**, *11* (12).
37. J. Yu, B. Luo, Y. Wang, S. Wang, K. Wu, C. Liu, S. Chu, H. Zhang; *Bioresour. Technol*., **2022**, *346*, 126640.
38. H. Yang, W. Yin, X. Zhu, P. J. Deuss, H. J. Heeres; *ChemCatChem*, **2022**, *14*, 20220097.

39. Y. Zheng, J. Wang, D. Li, C. Liu, Y. Lu, X. Lin, Z. Zheng; *J. Energy Inst*., **2021**, *97*, 58-72.
40. Y. L. Ding, H. Q. Wang, M. Xiang, P. Yu, R. Q. Li, Q. P. Ke; *Front Chem*, **2020**, *8*, 790.
41. M. Koehle, A. Mhadeshwar; *New Future Dev. Catal*., **2013**; 63-93.
42. J. Stetefeld, S. A. McKenna, T. R. Patel; *Biophys Rev*, **2016**, *8 (4)*, 409-427.
43. M. Kaszuba, D. McKnight, M. T. Connah, F. K. McNeil-Watson, U. Nobbmann; *J. Nanoparticle Res*., **2007**, *10 (5)*, 823-829.
44. J. Lim, S. P. Yeap, H. X. Che, S. C. Low; *Nanoscale Res. Lett*., **2013**, *8,* 381.